Journal of Ceramic Processing Research. Vol. 22, No. 4, pp. 409~420 (2021)
(Received 16 November 2020, Received in revised form 30 March 2021, Accepted 19 April 2021)
https://doi.org/10.36410/jcpr.2021.22.4.409

J O U R N A L O F
Ceramic Processing Research

Preparation and characterization of glass-ceramics with α-cordierite as the main crystalline phase from bluestone tailings

C.H. Li[a], W. Zhao[b,*], J.L. Zhang[a], W. Lu[b], P. Li[b], B.J. Yan[b] and H.W. Guo[b]
[a]*University of Science & Technology Beijing, Beijing 100083, China*
[b]*Soochow University, Suzhou 215006, China*

The bluestone tailings are quickly expanded in China with the continuous utilization and mining of bluestone resources. The incremental recycling of bluestone tailings is important to solve the resources waste and environmental pollution. This study aims to reuse the bluestone tailings as the main material to prepare α-cordierite glass-ceramics based on melting process. The results show that the nucleation temperature, crystallization peak temperature and the activation energy for crystallization decreased gradually with increasing the percentage of bluestone tailings. The complete preparation parameters of α-cordierite glass-ceramics include a bluestone tailings percentage of 70%, a heating rate of 5 $^{o}C \cdot min^{-1}$, a crystallization duration of 1.5 h, a crystallization temperature of 970 ^{o}C, a nucleation temperature of 830 ^{o}C, and a nucleation duration of 1.0 h. The performances analyses reveals that the α-cordierite glass-ceramics based on the optimized parameters exhibits high density and Vickers hardness, low dielectric loss and water absorption, and strong chemical resistance.

Keywords: cordierite glass-ceramics, bluestone tailings, crystallization kinetics, microstructure and phase transition.

Introduction

Bluestone is widely used as building materials and decorative materials due to its high bending strength, low water absorption, and great abrasive resistance [1, 2]. The bluestone body in Jiangxi, China consists of a slightly metamorphosed silt-bearing sericite slate of the Middle Proterozoic Shuangqiaoshan Upper Subgroup, and its exploitable deposits exceed 1.0×10^8 m^3 [3]. With continuous development and utilization of mining, the bluestone tailings wasteland is expanding quickly, not only occupying the large area land, but also being a serious contaminative source. Therefore, how to recycle the bluestone tailings incrementally is significant to solve the resources waste and environmental pollution.

Currently, the preparation of functional materials from solid wastes is considered as one of the most efficient and economical methods to solve the pollution problems caused by the solid wastes, such as metallurgical slag, tailings, coal gasification slag, fly ash, etc [4-8]. E. Fidancevska, R. Cimdins, T. Tomohiro, and A.A. Francis have used slag to prepare glass ceramics of CaO-MgO-Al_2O_3-SiO_2 (CMAS), i.e., glass-ceramics bearing silica fume and other crystalline phases, which shows a high mechanical strength [9-14]. He et al. illuminated the preparation of the glass-ceramics with diopside as the main crystalline phase from low and medium titanium-bearing blast furnace slag through melting methods, in which the mass percentage of titanium-bearing blast furnace slag is about 36% [15]. Overall, the total utilization rate of solid wastes is comparatively low in the preparation process of glass-ceramics. Yu et al. demonstrated that the single phase (α-cordierite) and low temperature co-fired cordierite-based glass-ceramics could be prepared from perlite tailings based on sintering methods [16, 17]. The cordierite-based glass ceramics are widely used as dielectric materials due to its high mechanical strength, low dielectric loss, and adjustable insulating coefficient [18-22]. Generally, the cordierite-based glass ceramics are designed with an approximate stoichiometric ratio 2 : 2 : 5 of MgO : Al_2O_3 : SiO_2. Besides, the nucleation agents and fluxing agents, such as TiO_2, P_2O_5, Li_2O, K_2O and Na_2O etc., are added to the cordierite-based glass ceramics system, aiming at decreasing the melting temperature and facilitate the crystallization process [23-25].

The chemical compositions of the bluestone tailings used in this study mainly consists of SiO_2, Al_2O_3, Fe_2O_3, K_2O and Na_2O, which indicates that the bluestone tailings are suitable for preparing cordierite-based glass ceramics after composition adjustment with MgO addition. The object of this article is to obtain the complete preparation parameters of α-cordierite glass-ceramics from bluestone tailings. Simultaneously, the effect of bluestone tailing percentage and heat treatment parameters on the crystallization behavior of α-cordierite glass-ceramics were illuminated systematically. Then, the properties of the prepared α-cordierite glass-

*Corresponding author:
Tel : +86-18202437339
Fax: +86-0512-67165621
E-mail: zhaowei0312@suda.edu.cn

ceramics were tested and compared with the traditional works. The results of this study could provide theoretical support for the high-efficiently utilization of bluestone tailings, and also introduce an innovative method to solve the resources waste and environmental pollution due to the huge storage of bluestone tailings.

Experimental

Raw materials and experimental design

The bluestone tailing used in this study was taken from a stone processing plant in Jiangxi, China, and its chemical compositions are listed in Table 1. The main components of the bluestone tailing are SiO_2, Al_2O_3, Fe_2O_3, K_2O and Na_2O. The sum of the SiO_2, MgO and Al_2O_3 content is more than 83%, and the sum of Fe_2O_3, K_2O and Na_2O content is up to 10.20%. In general, the SiO_2, MgO and Al_2O_3 are the main components of cordierite, and the Fe_2O_3 is widely used as nucleating agent in glass-ceramics preparation [26-28]. Besides, the introducing of alkali metal oxide in glass-ceramics could also decrease the viscosity of melted glass and the crystallization temperature. Therefore, it is suitable to apply the bluestone tailing as the main raw materials to prepare cordierite glass-ceramics.

For the cordierite system in reported literatures [29-30], the SiO_2-MgO-Al_2O_3 ternary phase diagram was determined, as shown in Fig. 1. In this study, the molar ratio of SiO_2, MgO and Al_2O_3 were controlled at 5 : 2 : 2 to guarantee the crystallizing of cordierite.

The detailed experimental design is listed in Table 2. The bluestone tailing percentage used in the preparation of glass-ceramics is controlled in the range from 40% to 70%. Also, the pure SiO_2, MgO and Al_2O_3 chemical reagent are added to guarantee the molar ratio of SiO_2, MgO and Al_2O_3 is 5 : 2 : 2. Note that the SiO_2 content has reached the maximum value in the cordierite system with the bluestone tailing percentage reaching 70%. Therefore, no extra SiO_2 reagent is required at the case of BT70.

The chemical compositions of the cordierite glass-ceramics with different bluestone tailing percentages are listed in Table 3. With a constant molar ratio of SiO_2: MgO: Al_2O_3 at 5:2:2, the content of SiO_2, MgO and Al_2O_3 ranges from 46.68%~48.69%, 12.32%~12.98%, and 31.84%~33.11%, respectively. With increasing the bluestone tailing percentage from 40% to 60%, the Fe_2O_3 content increases from 2.41% to 4.22%, and the total alkali metal oxides content, including Na_2O and K_2O, increases from 2.26% to 3.96%.

Preparation of glass-ceramics

In this study, the cordierite glass-ceramics were prepared *via* the melting method. The detailed preparation process mainly includes the following steps as shown in Fig. 2. Firstly, the raw materials, including bluestone

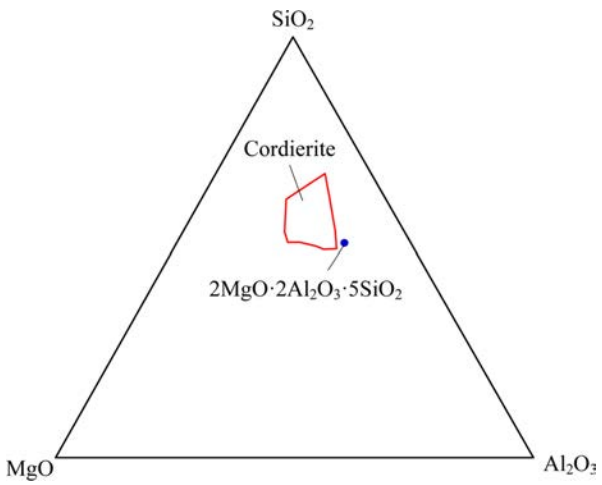

Fig. 1. SiO_2-MgO-Al_2O_3 ternary phase diagram.

Table 1. Chemical compositions of bluestone tailing (wt%)

SiO_2	MgO	Al_2O_3	CaO	K_2O	Na_2O	TiO_2	Fe_2O_3	Others
64.04	1.75	17.81	0.70	3.28	2.16	0.61	5.79	3.86

Table 2. Mass percentage of different raw materials used in the cordierite glass-ceramics preparation (wt%)

Case	Bluestone tailing	SiO_2	MgO	Al_2O_3
BT40	40.00	22.05	12.25	25.70
BT50	50.00	14.86	11.90	23.24
BT60	60.00	7.27	11.59	21.14
BT70	70.00	-	11.14	18.86

Table 3. Chemical compositions of cordierite glass-ceramics with different bluestone tailing ratios (wt%)

Case	Molar ratio (SiO_2:MgO:Al_2O_3)	SiO_2	MgO	Al_2O_3	Fe_2O_3	K_2O	Na_2O	CaO	TiO_2
BT40	5:2:2	48.69	12.98	33.11	2.41	1.36	0.90	0.29	0.20
BT50	5:2:2	48.17	12.81	32.50	3.01	1.71	1.12	0.36	0.32
BT60	5:2:2	47.24	12.68	32.26	3.61	2.05	1.35	0.44	0.38
BT70	5:2:2	46.68	12.32	31.84	4.22	2.39	1.57	0.51	0.44

Note: R_2O denotes the Na_2O and K_2O and other alkali metal oxide

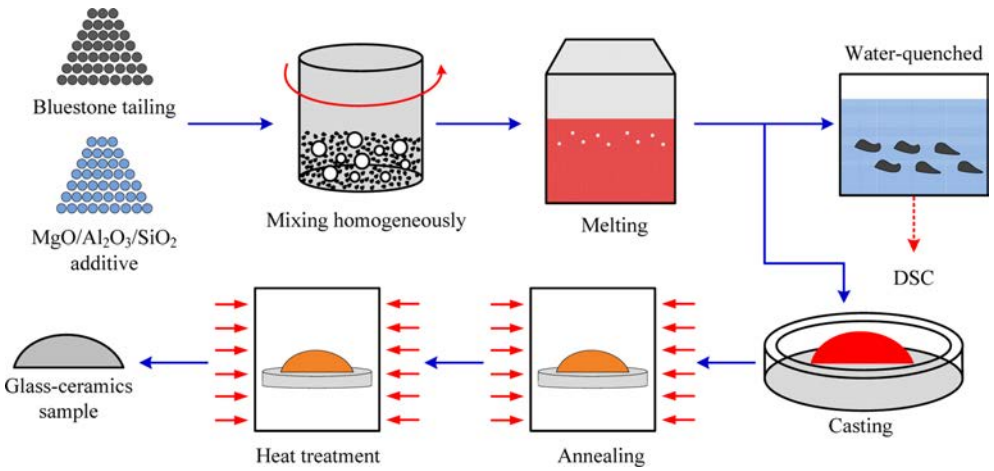

Fig. 2. Schematic diagram of cordierite glass-ceramics preparation process based on bluestone tailing.

tailing and pure chemical reagents, were mixed homogeneously with the pre-set mixing percentage in Table 2. The mixing process was conducted in the ball-milling machine with a ball-milling duration of 30 min, a ball-milling speed of 400 r/min, and a mass ratio of ball to material of 3.0. Next, the mixtures were charged into platinum crucible and heated in muffle furnace to 1,500 °C with a heating rate of 5 °C/min. Then, the mixtures were left at this temperature for 2 h until the material completely melted, and all bubbles disappeared. After that, a small part of the molten material was quenched with water, and the nucleation and crystallization temperatures were determined by Differential scanning calorimeter (DSC). The remaining samples were poured into a preheating mold, and then annealed at 600 °C. The heat treatment temperatures significantly affect the nucleation and crystallization of the glass-ceramics. In this study, the nucleation and crystallization temperatures are determined from the measured value of DSC curves. And the nucleation and crystallization duration are 1.0 h. After heat treatment, the glass-ceramic samples were cooled down to room temperature naturally in the furnace to release internal stress.

Characterization methods and performance testing

In this study, DSC technic was used to determine the nucleation and crystallization temperatures with a heating rate of 5, 10, 15, and 20 °C/min in nitrogen atmosphere (NETZSCH STA 449F5, NETZSCH, German). The crystalline phases were identified using X-ray diffraction (XRD, Ultima IV, Rigaku, Japan, Cu Kα, 10-90°) with a scanning speed of 2 °/min. The fractured surfaces of the glass-ceramic samples were chemically etched for 3-5 s in a 4 vol % HF solution to observe the microstructures using scanning electron microscopy (SEM, SU5000, Hitachi, Japan). Meanwhile, the elemental compositions were determined using energy-dispersive spectroscopy (EDS, X-MAX 20, Oxford, UK).

Results and Discussions

Crystallization kinetics evaluation

The non-isothermal DSC curves of the parent glass at different bluestone tailings percentages and heating rates are shown in Fig. 3. The exothermic peaks in DSC curves imply the occurrence of nucleation and crystallization in the heat treatment process. When the heating rate is 10 °C·min^{-1}, the nucleation temperature T_g and crystallization temperature T_p decreased from 836.5 °C and 996.1 °C to 823.1 °C and 976.7 °C with the bluestone tailings percentage increased from 40% to 70%. This indicates that the bluestone tailings addition could reduce the superheating required for nucleation and crystallization, thereby promoting low-temperature crystallization. Besides, the T_g and T_p for each case shifted towards higher temperatures at a greater heating rate due to the hysteretic nature of the heat effect.

The non-isothermal crystallization kinetics could be described using the Kissinger equation as follows:

$$\ln(T_p^2/\alpha) = E_c/(RT_p) + \ln(E_c/R) - \ln v \quad (1)$$

where α is the heating rate (K/s), R is the gas constant (8.314 J·mol^{-1}·K^{-1}), E_c is the activation energy of crystallization (J·mol^{-1}), and v is the pre-exponential factor.

Fig. 4 shows the plot of $\ln(T_p^2/\alpha)$ versus $10000/T_p$ at different bluestone tailings percentages. The activation energy Ec and pre-exponential factor v could be calculated by the slope Ec/R and intercept ($\ln(Ec/R)$-$\ln v$) of the fitted line in Fig. 2. The Avrami parameters n is employed as an interpretation of the crystallization mechanism [31], and it can be calculated from the Augis-Bennett equation [32-33] as follows:

$$n = \frac{2.5T_p^2}{\Delta T_f \, E_c/R} \quad (2)$$

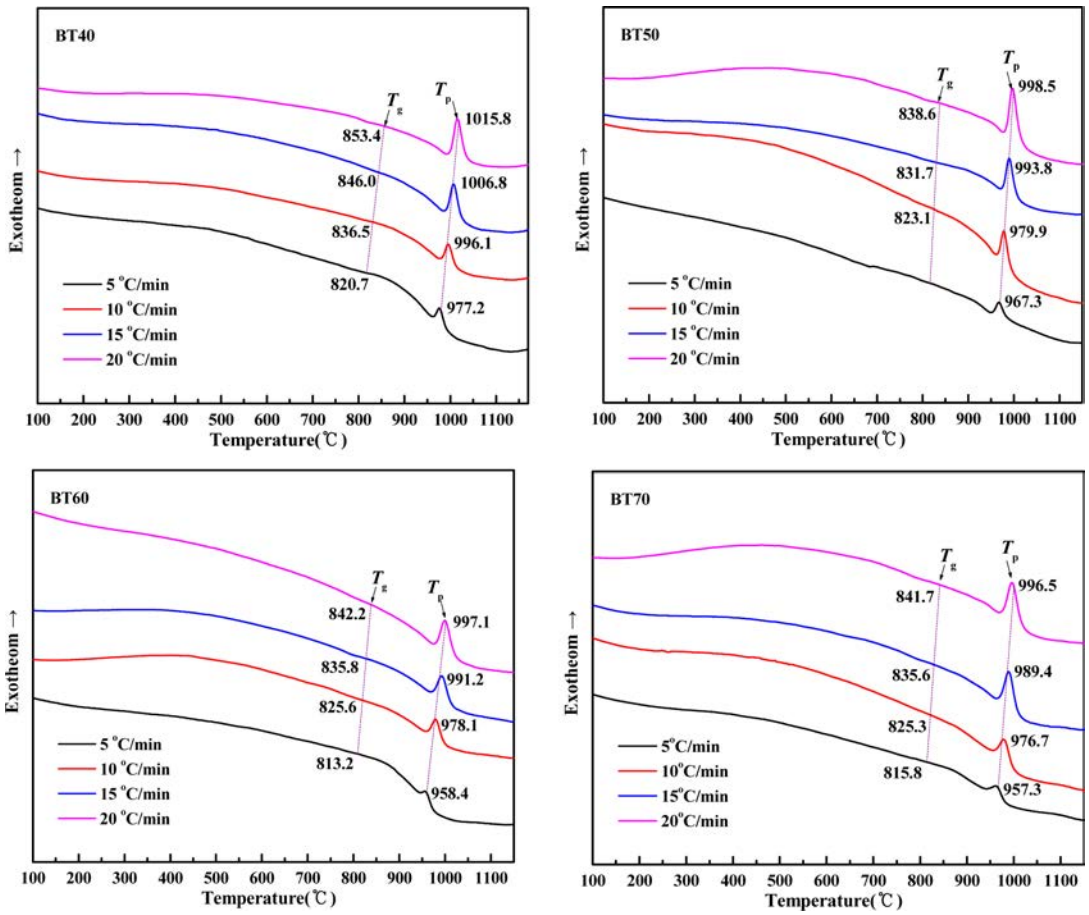

Fig. 3. DSC curves of the parent glass samples BT40-BT70 at various heating rates.

Table 4. Activation energy, pre-exponential factor and Avrami parameters of the parent glass samples BT40-BT70

Case	Activation energy *Ec* (kJ·mol^{-1})	pre-exponential factor *v* (min^{-1})	Avrami parameters *n*			
			5 °C/min	10 °C/min	15 °C/min	20 °C/min
BT40	463.52	4.14×10^{15}	3.79	3.74	3.57	3.55
BT50	440.16	3.02×10^{15}	4.28	4.12	3.92	3.62
BT60	434.25	4.49×10^{14}	4.45	4.43	4.36	4.24
BT70	432.77	4.05×10^{14}	4.76	4.68	4.54	4.54

Where ΔT_f is the full width at half maximum of the exothermic peak. The Avrami parameters at different heating rates are listed in Table 4. It can be seen that the activation energy decreased from 463.52 kJ·mol^{-1} to 432.77 kJ·mol^{-1} obviously with increasing the bluestone tailings percentage from 40% to 70%. This indicates that the increasing of bluestone tailings could facilitate the crystallization through a lowered activation energy. The Avrami parameters increased gradually with enhancing the bluestone tailings percentage, which indicates that the bluestone tailings could improve the crystallization ability of the base glass. In addition, the Avrami parameters mainly ranged from 3.0 to 5.0 and the volume crystallization could be occurred, which benefits to prepare the glass-ceramics samples with higher density and better performances.

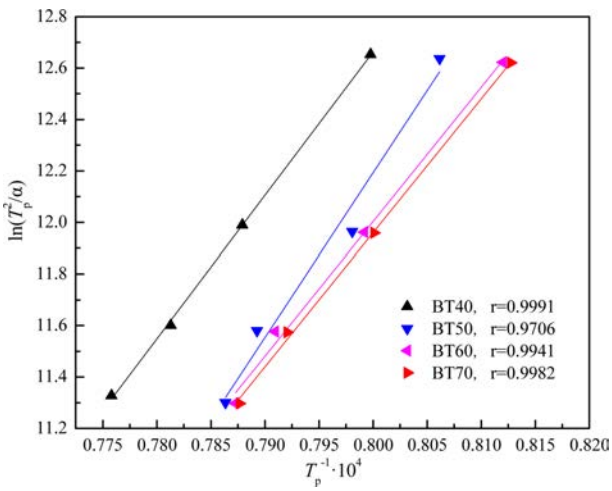

Fig. 4. Plots of $\ln(T_p^2/\alpha)$ *vs* $10000/T_p$ for the parent glass samples BT40-BT70.

Effect of bluestone tailings percentage on the phase and microstructure of glass-ceramics

Based on the abovementioned nucleation and crystallization temperature, the preliminary heat treatment parameters, including T_g, T_p, nucleation duration, crystallization duration, and heating rate are listed in Table 5. After heat treatment, the glass-ceramics samples were analyzed by XRD and SEM-EDS.

Fig. 5 shows the XRD patterns and crystallinity of glass-ceramics with different bluestone tailing percentages. As shown in Fig. 5(a), the main crystal phases in the different glass-ceramics samples are α-cordierite ($Mg_2Al_4Si_5O_{18}$, PDF : 82-1884), and there are no γ-cordierite peaks observed. With increasing the bluestone tailing percentages, the diffraction peaks of α-cordierite increased obviously at the crystal orientation of (010), (012), (112), (121), and (022), which indicates the enhancing of bluestone percentage could promote the precipitation and growth of α-cordierite crystals effectively. Further, the crystallinities of the samples were calculated by the Jade software using Rietveld refinement [34, 35] and the results are shown in Fig. 5(b). It can be found that the increasing of bluestone tailings from 40% to 60% lead to an obviously crystallinity increasing from 49% to 64%. Therefore, the increasing of bluestone tailings could promote the crystallization of α-cordierite glass-ceramics.

The microstructures and EDS results of the glass-ceramics with different bluestone tailings percentages after chemically etched are shown in Fig. 6. The objective of the chemically etching is to remove the glass matrix effectively and observe the crystal particles clearly. It can be seen that large amounts crystal particles precipitated in the different glass-ceramics samples. The EDS results of the crystals show that the stoichiometric ratio of Si: Mg: Al is about 5:2:4, which indicates the cordierite is the main crystal phase. In the case BT40 and BT50, the crystal particle size is higher than 2 μm. Simultaneously, there are several pores generated in the two samples, which is mainly due to the crystallinity is relative lower and the glass matrix could be etched significantly. With increasing the bluestone tailings, the crystal particle size gradually becomes smaller, and the average crystal particle size is about 1.5 μm in case BT70, as shown in Fig. 6(d). Besides, in the case BT60 and BT70, the pores disappeared due to the crystallinity increasing, which could be attributed to the increased K and Fe content with enhancing the bluestone tailings. Considering the fully utilization of the bluestone tailings, the recommended bluestone tailings percentage is 70% in the glass-ceramics preparation.

Table 5. The preliminary heat treatment parameters of glass-ceramics with different bluestone tailings percentages

Case	T_g/°C	Nucleation duration/h	T_p/°C	Crystallization duration/h	Heating rate/ °C·min^{-1}
BT40	840	1.0	1000	1.0	10
BT50	830	1.0	980	1.0	10
BT60	830	1.0	980	1.0	10
BT70	830	1.0	980	1.0	10

Optimization of heat treatment parameters

Based on the abovementioned bluestone tailings percentage, nucleation temperature and nucleation duration, the heat treatment parameters were optimized by single-factors experiments. The detailed levels of the selected factors, including crystallization temperature, crystallization duration, and heating rate, are listed in Table 6.

The XRD patterns and crystallinity of the glass-ceramics with different heating rate are shown in Fig. 7. As shown in Fig. 7(a), the main crystal phases with the different heating rate are α-cordierite, and with enhancing the heating rate, the diffraction peaks of α-cordierite decreased slightly at the crystal orientation of (121), and (022), which indicates the enhancing of heating rate could restrain the precipitation and growth

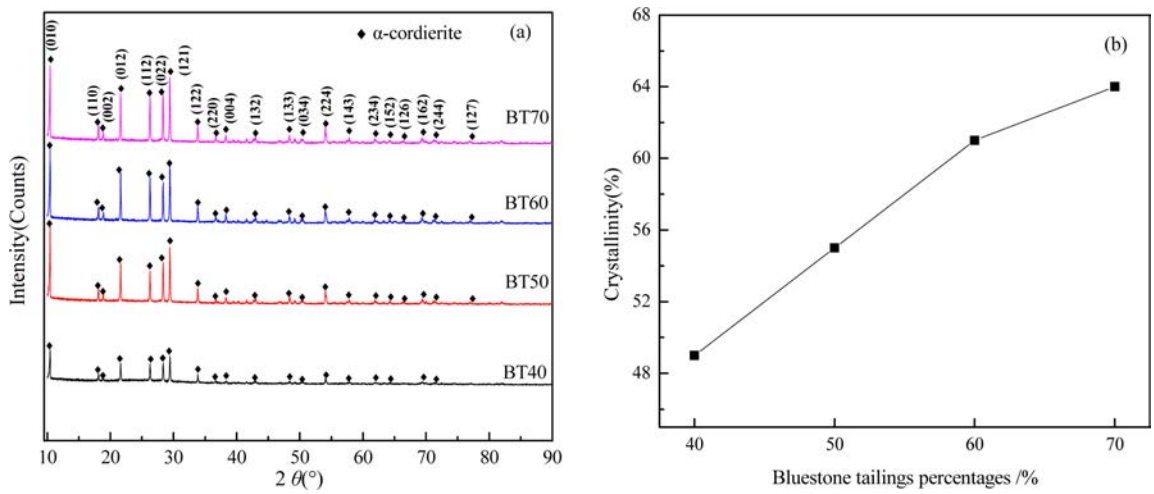

Fig. 5. XRD patterns (a) and crystallinity (b) of glass-ceramics with different bluestone tailing percentages.

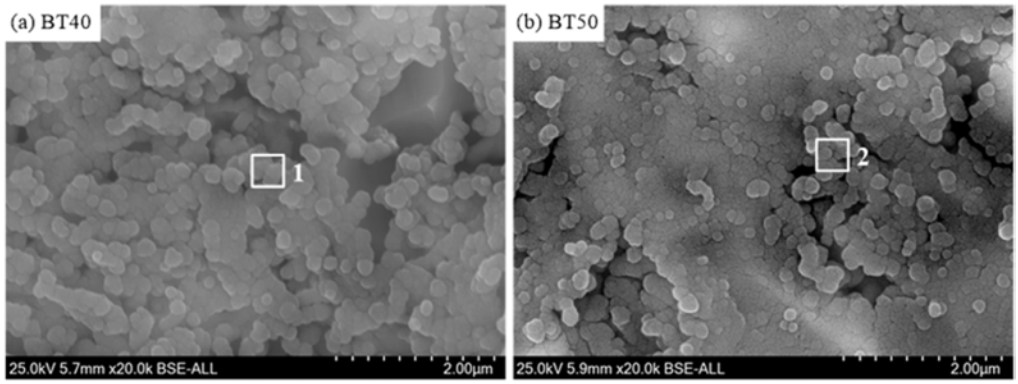

Point	Ca	Si	Mg	Al	O	K	Na	Ti	Fe
1	2.3	24.9	12.2	24.5	28.0	2.0	2.2	0.4	3.5
2	3.8	23.5	10.4	21.4	32.6	2.0	2.6	0.4	3.2
3	1.3	25.9	7.6	20.5	33.5	3.3	1.6	0.7	5.5
4	1.4	23.0	6.4	20.3	36.7	3.5	2.0	0.5	6.2

Fig. 6. SEM-EDS of the glass-ceramics with different bluestone tailings percentages after chemically etched.

Table 6. The preliminary heat treatment parameters of glass-ceramics with different bluestone tailings percentages

Factors	Levels				
Crystallization temperature / °C	910	930	950	970	990
Crystallization duration /h	0.5	1.0	1.5	2.0	
Heating rate /°C·min^{-1}	2	5	8	11	
Nucleation temperature / °C	830				
Nucleation duration /h	1.0				

of α-cordierite crystals. The crystallinities of the samples, as shown in Fig. 7(b), decreased from 65% to 57% with lowering the heating rate from 11 °C·min^{-1} to 2 °C·min^{-1}. This is because a lower heating rate indicates a longer crystal growth time, thereby facilitating the crystallization ability.

The heating rate has a significantly effect on the growth and aggregation of the crystal particle, as shown in Fig. 8. With a heating rate of 2°C·min^{-1} and 5°C·min^{-1}, the α-cordierite crystal particles distributed uniformly and the particle size mainly ranged from 0.5μm to 1.5μm, as shown in Fig. 8(a) and 8(b). With increasing the heating rate to 8°C·min^{-1} and 11°C·min^{-1}, the particle size of most crystals was higher than 2.0μm, and the aggregation phenomenon of the crystal particle was more serious than that with a lower heating rate, which is due to the fact that the increasing of the heating rate could reduce the nucleation points, thereby decreasing the amounts of crystal particles and increasing the particle size. Therefore, fully considering the crystallinity, energy consumption and preparation efficient of the glass-ceramics, the selected heating rate is 5°C·min^{-1}.

The XRD patterns and crystallinity of the glass-ceramics with different heating rate are shown in Fig. 9. As shown in Fig. 9(a), the main crystal phases at different crystallization temperatures are α-cordierite, and the peaks intensity increased obviously with enhancing the crystallization temperature. At 910 °C, the peaks intensity of α-cordierite phase was lower, and an obvious bread peak could be observed with a diffraction angle ranging from 20°~30°, which indicates that the crystallization is insufficient and the crystallinity is as low as 37.0%.

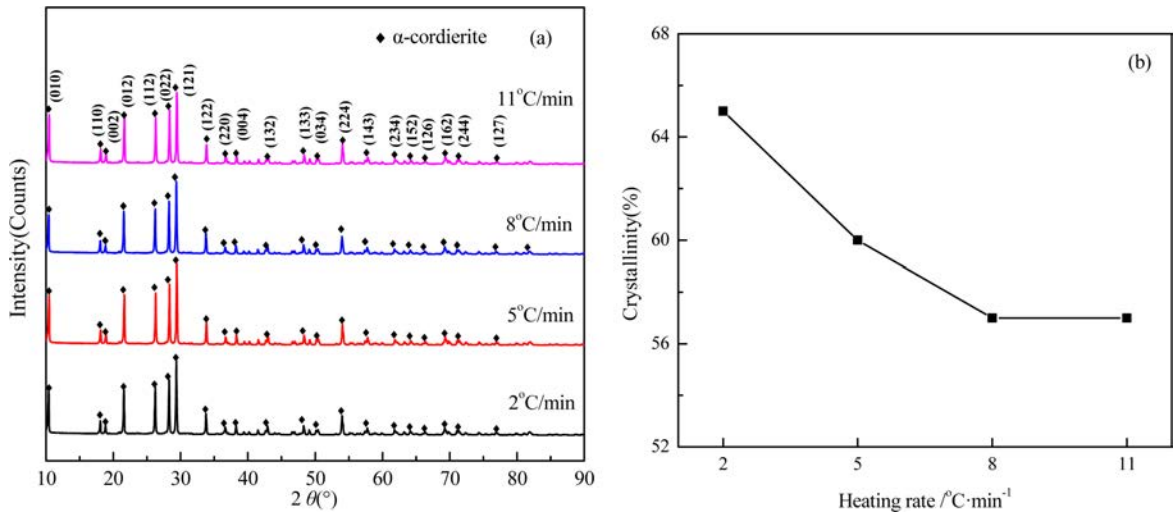

Fig. 7. XRD patterns (a) and crystallinity (b) of glass-ceramics with different heating rate.

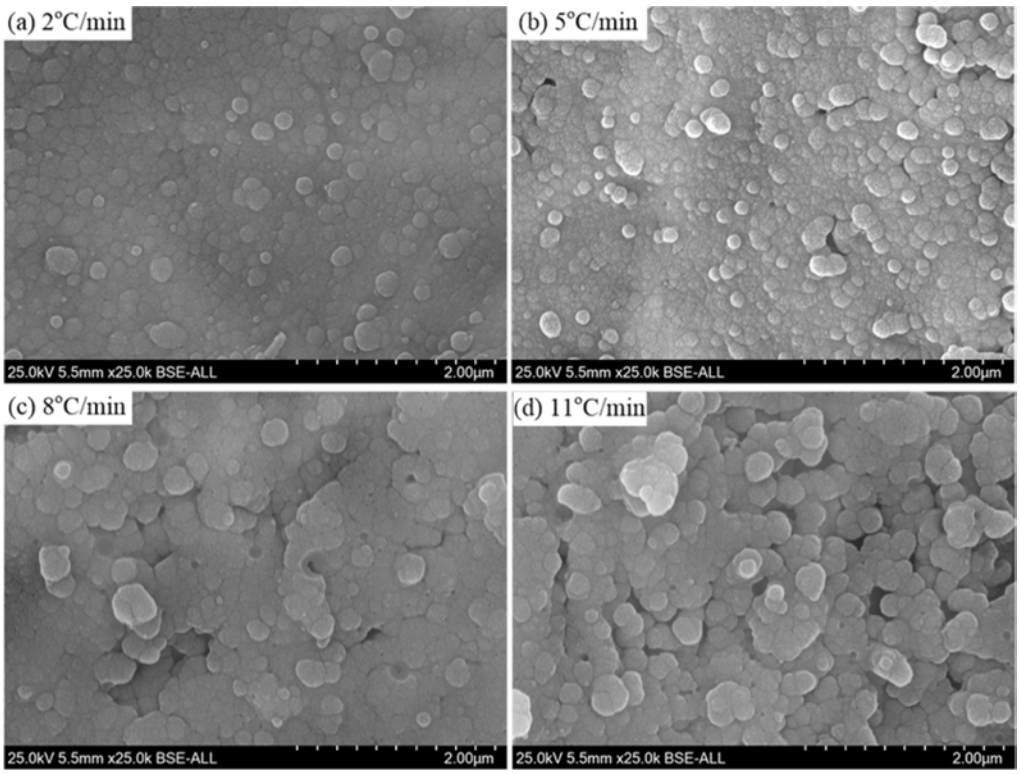

Fig. 8. Microstructures of the glass-ceramics with different heating rate after chemically etched.

With increasing the crystallization temperature from 910 ºC to 970 ºC, the diffraction peaks of α-cordierite increased obviously at the crystal orientation of (010), (012), (112), (121), and (022), which indicates the enhancing of crystallization temperature could promote the precipitation and growth of α-cordierite crystals effectively. Correspondingly, the crystallinity increased and reached the maximum value 64% at 970 ºC, as shown in Fig. 9(b). With further increasing the temperature to 990ºC, the crystallinity decreased slightly, which is mainly caused by the remelting of some crystals at this temperature.

Fig. 10 shows the microstructures of the glass-ceramic samples prepared at different crystallization temperature. As shown in Fig. 10(a), a lot of cracks appeared in the glass-ceramics, which could be attributed to the following reasons. (1) With a crystallization temperature of 910 ºC, the crystallinity was relatively low and large amounts glass phases existed. In the cooling process, the different expansion properties between glass phases and crystal phases would result in the internal stress and produce fine cracks. (2) To

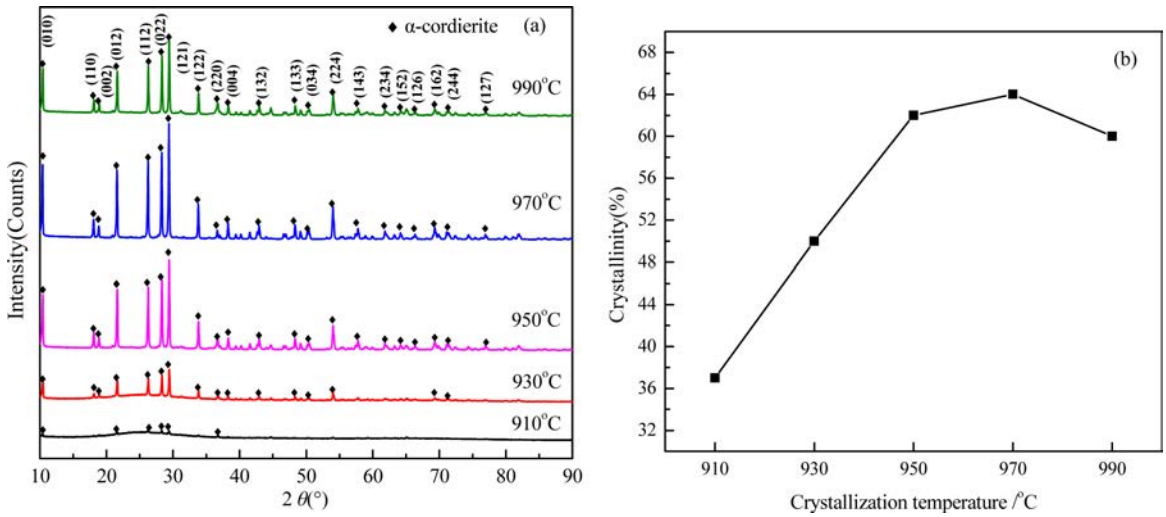

Fig. 9. XRD patterns (a) and crystallinity (b) of glass-ceramics with different crystallization temperature.

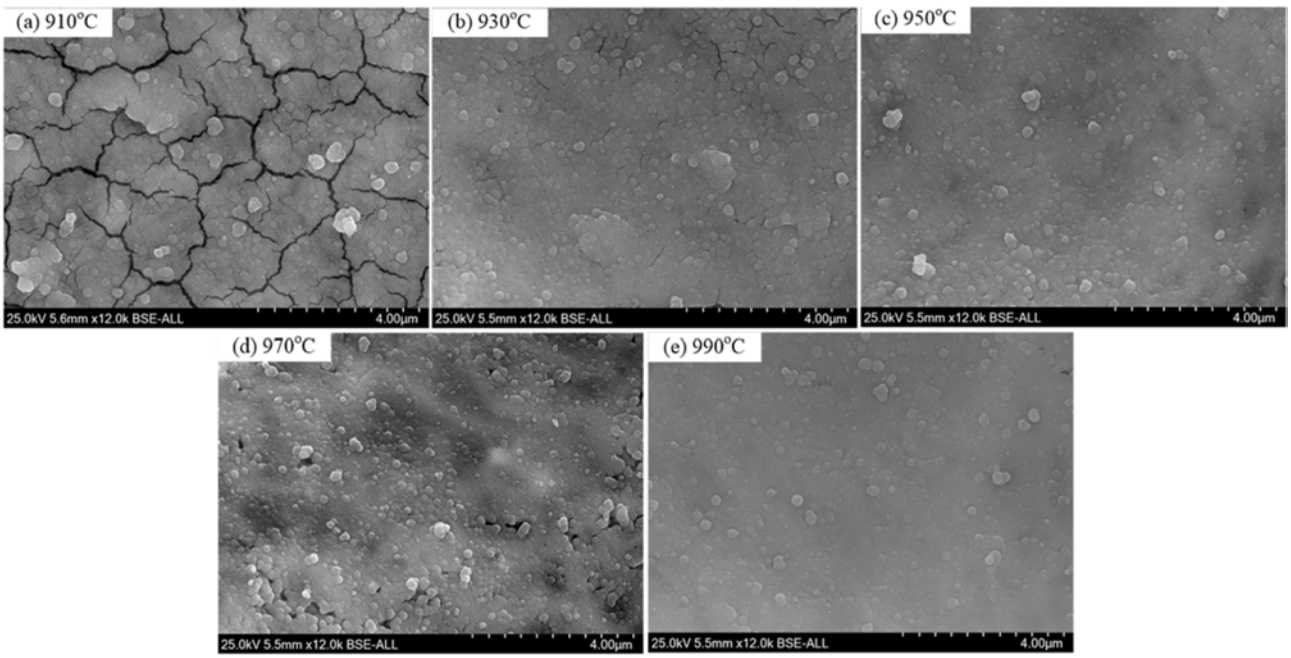

Fig. 10. Microstructures of the glass-ceramics with different crystallization temperature after chemically etched.

observe the crystals in glass-ceramics, the samples were chemically etched for 3-5 s in a 4 vol % HF, which would dissolve the glass phase and promote the cracks growth further. With increasing the crystallization temperature, the crystallinity increased and the cracks gradually disappeared. With increasing the crystallization temperature to 990 ºC, the crystal grain edges became blurred, which indicates that the remelting of crystal grains occurred gradually. As a result, the crystallinity of glass-ceramics reduced slightly. Therefore, considering the crystallinity and microstructures of the glass-ceramics, the recommended crystallization temperature is 970 ºC.

Fig. 11 shows the XRD patterns and crystallinity of the glass-ceramics with different crystallization duration. It can be seen that the main components in the glass-ceramics is α-cordierite. With the increase of crystallization duration, the diffraction peaks of α-cordierite increased at the crystal orientation of (010), (012), (112), (121), and (022). This indicates the increase of crystallization duration could promote the precipitation and growth of α-cordierite crystals obviously. Simultaneously, the calculated crystallinity increased obviously from 52% to 65% with increasing the crystallization duration from 0.5 h to 1.5 h, and then increased slightly to 66% with further increasing the crystallization duration to 2.0h. This indicates that the increasing of crystallization duration could facilitate the crystallization of bluestone tailing glass-ceramics. Fully considering the crystallinity tendency and the energy consumption, the selected

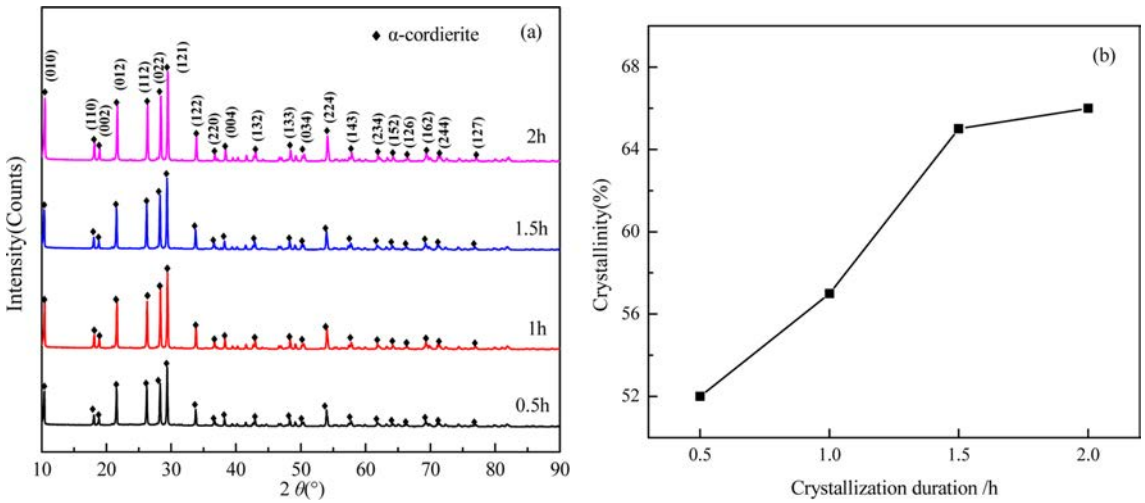

Fig. 11. XRD patterns (a) and crystallinity (b) of glass-ceramics with different crystallization duration.

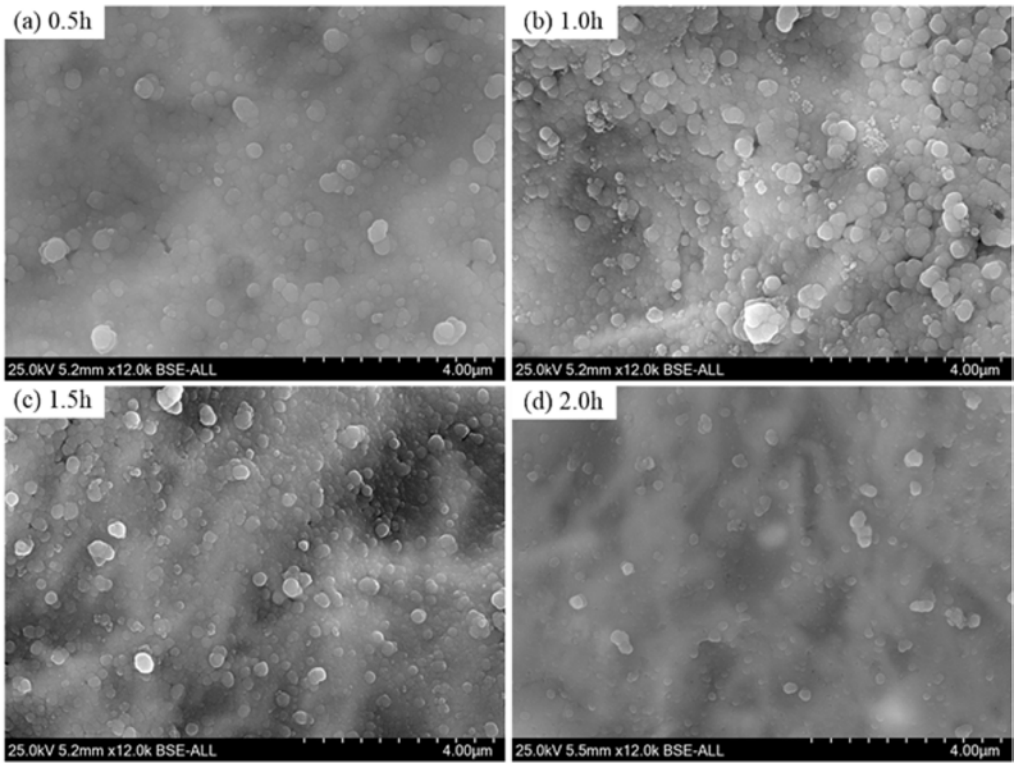

Fig. 12. Microstructures of the glass-ceramics with different crystallization duration after chemically etched.

crystallization duration is 1.5 h.

Fig. 12 shows the microstructures of the samples prepared at different crystallization duration. At 0.5 h, the crystal particle size is smaller than 2 μm, and large amounts glass phases could be observed due to the low crystallinity, as shown in Fig. 12(a). With increasing the heat treatment duration, the glass phases gradually disappeared and the crystals growth, the particle size of most crystals is larger than 2 μm when the crystallization duration is 2.0 h, as shown in Fig. 12(d). Notably, the crystal distribution and particle size are relatively more uniform in Fig. 12(c) than that in the other cases. Therefore, based on the abovementioned results, the recommended heat treatment parameters include a heating rate of 5 ºC·min^{-1}, a crystallization duration of 1.5 h, a crystallization temperature of 970 ºC, a nucleation temperature of 830ºC, and a nucleation duration of 1.0 h.

To illustrate the nucleation and crystallization mechanism of the cordierite glass-ceramics prepared from bluestone tailings, the structures of the glass-ceramics at nucleation and crystallization stage are shown in Fig. 13. The structures transitions during heat treatment could be divided into three stages, namely the nucleation stage, nucleation and growth stage, and crystallization and

growth stage. The transition stages closely related to the nucleation temperature (T_g) and crystallization temperature (T_p). With increasing the temperature to T_g, the crystal nucleus began to precipitate in the sample, as shown in Fig. 13(a). In the temperature range from T_g to T_p, the new crystal nucleuses are continuously formed in the sample. Simultaneously, the crystal nucleuses formed earlier begin to grow due to temperature increasing, as shown in Fig. 13(b). With increasing the temperature to T_p, the crystal nuclei formed in the sample earlier begin to grow uniformly, as shown in Fig. 13(c).

Property evaluation

The glass-ceramics sample prepared with different bluestone tailings under a heating rate of 5 ºC·min^{-1}, a crystallization duration of 1.5 h, a crystallization temperature of 970 ºC, a nucleation temperature of 830 ºC and a nucleation duration of 1.0 h were used for properties testing. The density, Vickers hardness, and dielectric loss of the glass-ceramic sample were tested, and the results are shown in Fig. 14. It can be seen that the density and Vickers hardness are increased with enhancing the bluestone tailings percentage. This may be related to the improved crystallinity and grain refinement and homogenization. With a bluestone tailings percentage of 70%, the density and the Vickers hardness are 2.89 g·cm^{-3} and 813.23 HV, which are similar to those for cordierite-based glass-ceramics as obtained from the previous research [5]. The dielectric properties, including dielectric constant and dielectric loss, were tested at a frequency of 10MHz. As shown in Fig. 14, the dielectric constant and dielectric loss increased slightly with increasing the bluestone tailings percentage. The dielectric constant and dielectric loss are mainly ranging from 15 to 17 and 0.01 to 0.03 and obviously higher than that in the reported researches [11], which is mainly caused by the higher alkali metals content

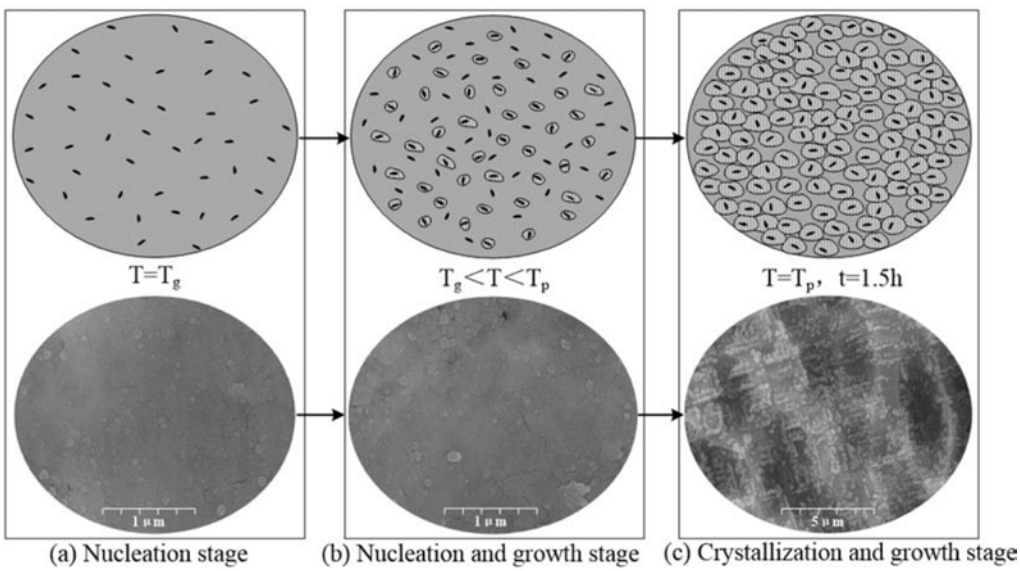

Fig. 13. Schematic diagram of the glass-ceramic nucleation and crystallization stage during heat treatment.

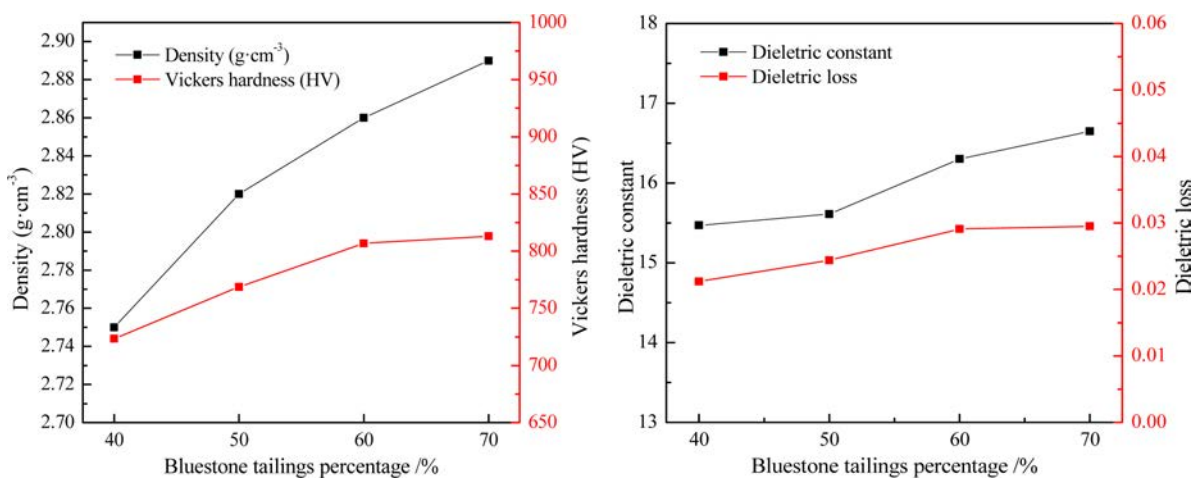

Fig. 14. The properties of glass-ceramics with different bluestone tailings percentages.

Table 7. The water absorption and chemical resistance of the glass-ceramics with different bluestone tailings percentages

Bluestone tailings percentage /%	Water absorption /%	Chemical resistance	
		1 vol% H_2SO_4	1 wt.% NaOH
40	0.46	0.06	0.07
50	0.37	0.03	0.06
60	0.32	0.04	0.03
70	0.30	0.02	0.02

(K_2O, Na_2O, Fe_2O_3) in the bluestone tailings.

Besides, the water absorption and chemical resistance of the glass-ceramics with different bluestone tailings percentages are listed in Table 7. With increasing the bluestone tailings percentages, both the water absorption and chemical resistance decreased obviously, which are mainly caused by the improved densification and high crystallinity. In conclusion, the bluestone tailings could promote the crystallization and decrease the pores, thereby inhibiting the absorption or erosion process.

Conclusions

(1) With increasing the bluestone tailings percentage from 40% to 70%, the crystallization activation energy decreased from 463.52 $kJ \cdot mol^{-1}$ to 432.77 $kJ \cdot mol^{-1}$ obviously, and the Avrami parameters enhanced gradually in the range from 3.0 to 5.0, which indicates that the increasing of bluestone tailings could facilitate the crystallization of the base glass.

(2) With a bluestone tailings percentage of 70%, the optimized preparation parameters of α-cordierite glass-ceramics include a heating rate of 5 $^{o}C \cdot min^{-1}$, a crystallization duration of 1.5 h, a crystallization temperature of 970 ^{o}C, a nucleation temperature of 830 ^{o}C, and a nucleation duration of 1.0 h.

(3) The performances analysis reveals that the α-cordierite glass-ceramics based on the optimized parameters exhibits high density, Vickers hardness, and dielectric loss. Simultaneously, the high crystallinity and the improved the densification and inhibiting the absorption or erosion process.

Acknowledgements

The authors are especially thankful to Project of Transformation of Scientific and Technological Achievements of Inner Mongolia Autonomous Region (2019CG073), National Natural Science Foundation of China (51574169), Natural Science Research Project of Higher Education in Jiangsu Province (20KJB45002), and Postdoctoral Research Foundation of Jiangsu Province (7114451120).

References

1. T.M. Zhang, Jiangxi Geology. 13[3] (1999) 194-199.
2. X. Dong, in "Environmental performance analysis of construction waste regeneration" (Shandong University of Science and Technology, 2011) p.8-13.
3. C. Liu, in "A study on the all-around effect evaluation & countermeasure analysis of mineral's exploitation in Xingzi region on the south of Lushan mountain" (China University of Geosciences, 2004) p.9-15.
4. H.D. Yuan, H.F. Yin, Y. Tang, Y.L. Xin, X.L. Pu, and H. Zhang, J. Ceram. Process. Res. 21[6] (2020) 640-646.
5. W. Dang and H.Y. He, J. Ceram. Process. Res. 21[1] (2020) 69-74.
6. S. Lamprakopoulosa, V. Karayannisb, G. Papapolymeroua, D. Kasiteropouloua, K. Ntampegliotisa, and X. Spiliotisa, J. Ceram. Process. Res. 17[9] (2016) 985-989.
7. M.L. Öveçoğlu, B. Kuban, and H. Özer, J. Eur. Ceram. Soc. 17[7] (1997) 957-962.
8. E. Karamanova, G. Avdeev, and A. Karamanov, J. Eur. Ceram. Soc. 31[6] (2011) 989-998.
9. R. Cimdins, I. Rozenstrauha, L. Berzina.L, J. Bossert, and M. Bucker, Resour. Conserv. Recycl. 29[4] (2000) 285-290.
10. T. Toya, Y. Kameshima, A. Yasumori, and K. Okada, J. Eur. Ceram. Soc. 24[8] (2004) 2367-2372.
11. A.A. Francis, J. Eur. Ceram. Soc. 24[9] (2004) 2819-2824.
12. J.R. Wu, A.R. Boccaccini, R.D. Lee, and R.D. Rawlings, Glass Technol.Part A Eur. J. Glass Sci. Technol. 48[3] (2007) 133-141.
13. H. Elsayed, A. Zocca, E. Bernardo, C.M. Gomes, J. Gunster, and P. Colombo, J. Eur. Ceram. Soc. 35[2] (2015) 731-739.
14. J.S. Cheng, H. Li, and L.Y. Tang, in "Glass-ceramics" (Chemical Industry Press, 2006) p.1.
15. D.F. He, C. Gao, J.T. Pan, and A.J. Xu, Ceram. Int. 44[2] (2018) 1384-1393.
16. Y.S. Yu, X.F. Hao, L.X. Song, Z. Li, and L. Song, J. Non-Cryst. Solids 448 (2016) 36-42.
17. S. Li, J.F. Wu, Z. Li, X.F. Hao, and Y.S. Yu, J. Non-Cryst. Solids 419 (2015) 16-26.
18. Z. Li, J. Wu, L. Song, and Y.Q. Huang, J. Eur. Ceram. Soc. 34[15] (2014) 3981-3991.
19. S.P. Hwang and J.M. Wu, J. Am. Ceram. Soc. 84[5] (2010) 1108-1112.
20. S. Kumar and B.B. Nag, J. Am. Ceram. Soc. 49[1] (2010) 10-14.
21. F. Liu, X.P. Huang, J.J. Qu, C.L. Yuan, G.H. Chen, and R.F. Ma, J. Non-Cryst. Solids 481 (2018) 329-334.
22. M. Dittmer, C.F. Yamamoto, C. Bocker, and C. Russel, Solid State Sci. 13[12] (2011) 2146-2153.
23. S. Jo and S. Kang, J. Nanosci. Nanotechnol. 13[5] (2013) 3542-3545.
24. J.M. Wu and S.P. Hwang, J. Am. Ceram. Soc. 83[5] (2000) 1259-1265.
25. K. Sumi, Y. Kobayashi, and E. Kato, J. Am. Ceram. Soc. 82[3] (2010) 783-785.
26. P. Alizadeh, B.E. Yekta, and A. Gervei, J. Eur. Ceram. Soc. 24[13] (2004) 3529-3533.
27. M.Z. Zhao, J.W. Cao, X.H. Geng, W.F. Song, and Z. Wang, J. Non-Cryst. Solids 547 (2020) 120295.
28. N.O. Dantas, W.E.F. Ayta, A.C.A. Silva, N.F. Cano, S.W. Silva, and P.C. Morais, Spectroc. Acta Pt. A-Molec. Biomolec. Spectr. 81[1] (2011) 140-143.
29. N. Obradovic, V. Pavlovic, M. Kachlik, K. Maca, D. Olcan, A. Dordevic, A. Tshantshapanyan, B. Vlahovic, and V. Pavlovic, Adv. Appl. Ceram. 118[5] (2019) 241-248.
30. Y.H. Pan, P.F. Zhu, R. Wang, Z.C. Si, B. Li, and Y.W. Yao, Ceram. Int. 45[12] (2019) 15230-15236.

31. H. Hosono and Y. Abe, Mater. Res. Bull. 29[11] (1994) 1157-1160.
32. K. Matusta, T. Komatsu, and R. Yokota, J. Mater. Sci. 19 [1] (1984) 291-296.
33. J.A. Augis and J.E. Benett, J. Therm. Anal. 13[2] (1978) 283-292.
34. F.C. Serbena, V.O. Soares, O. Peitl, H. Pinto, R. Muccillo, and E.D. Zanotto, J. Am. Ceram. Soc. 94[4] (2011) 1206-1214.
35. M. Dittmer, C. Ritzberger, M. Schweiger, V. Rheinberger, M. Wörle, and W. Höland, J. Non-Cryst. Solids 384 (2014) 55-60.